CONSTRUCTION MATERIALS CONSULTANTS, INC.

Laboratory Studies of A Concrete Cylinder To Investigate Lower-Than-Design Compressive Strength of Concrete

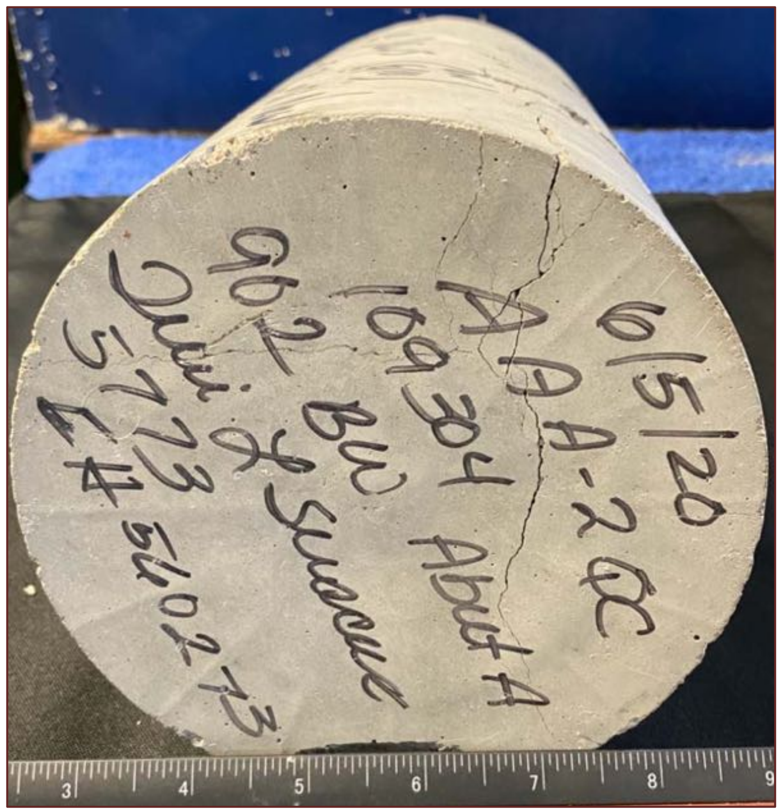

July 2, 2020
CMC 0620127

TABLE OF CONTENTS

Further Study:

Jana, D., Erlin, B., and Pistilli, M.F., "A Closer Look at Entrained Air in Concrete," *Concrete International*, July 2005, pp. 31-34.

EXECUTIVE SUMMARY

The purpose of this study is to investigate lower-than-design compressive strength issue of concrete. The concrete in question is reported to be representative of a mix design of PennDOT AAA, which contains (in a cubic yard): 600 pounds of ASTM C 150 Type II Portland cement, 150 pounds of ASTM C 618 Class F fly ash (i.e. 20 percent fly ash addition by mass of total cementitious materials), 1678 pounds of #57 crushed stone coarse aggregate, 1094 pounds of concrete sand, 337 pounds of water, Sika Plastocrete 250 @ 5 oz/cwt of total cementitious materials, Sika Viscocrete 1000 @ 1 oz/cwt of total cementitious materials, Sika AEA @ 1 oz/cu. yd. all to comply with PennDOT AAA Mix design having a design water-cementitious materials ratio of 0.45, a 28-day design strength of 4000 psi, and a design weight of 142.4 pounds per cubic yard. According to PennDOT Specification 704, the range of design air content is from 3.5 to 7.5 percent.

A concrete cylinder identified as AAA-2QC was provided for examinations, which was previously tested for compressive strength and produced a strength of 2960 psi in 6 days of curing, which is within the anticipated strength for its age for a 4000 psi design mix. The cylinder was tested according to the procedures of ASTM C 856 "Standard Practice For Petrographic Examination of Hardened Concrete." Based on detailed petrographic examinations, concrete in the cylinder is found to contain: (a) crushed greywacke coarse aggregate having a nominal maximum size of 1 in. (25 mm), which are argillaceous sandstone consisting of detrital quartz-quartzite-feldspar grains in an argillaceous (sericitic clay-based) matrix; (b) natural siliceous-argillaceous sand fine aggregate having a nominal maximum size of $^3/_8$ in. (9.5 mm) and containing major amounts of quartz, quartzite, feldspar particles, and subordinate amounts of chert, shale, and siltstone particles, etc., (c) a dense hardened paste containing major amounts of Portland cement and subordinate amount of fly ash having a total cementitious materials content estimated to be equivalent to $7^1/_2$ to 8 bags of Portland cement per cubic yard of which 20 percent is estimated to be fly ash, (d) a water-cementitious materials ratio estimated to be 0.40 to 0.45, and (e) an air content estimated to be 8 to 10 percent, which is higher than the maximum design air content of 7.5 percent.

In order to further investigate the actual air content, a detailed air-void analysis of concrete according to the modified point count procedure of ASTM C 457 was conducted, which has produced an air content of 8.1 percent, a void frequency of 29.68/in., an air-void specific surface of 1463 in^2/in^3 and a void spacing factor of 0.0029 in. Air-void parameters are indicative of a very 'fine' air-void system of high specific surface (noticeably higher than the common industry-recommended minimum value of 600 in^2/in^2) but an excessively air-entrained concrete that has numerous fine discrete spherical entrained voids to provide the necessary freeze-thaw durability of concrete but have more than necessary air to negatively affect the compressive strength. Although the 6-day strength result of this particular cylinder do not show any negative effect, such high air can explain the reported inconsistent strength results throughout the project.

Along with high air, a side effect of having a lot of very fine air bubbles e.g., from uncontrolled dosages of air-entraining chemical is clustering of air voids especially along aggregate-paste interfaces to create a frothy-textured paste in the aggregate sockets, which reduces the aggregate-paste bond, and, thereby, reduces the compressive strength of concrete. The present cylinder showed such evidence of air-void clustering along the interfaces between crushed greywacke coarse aggregate particles and mortar fraction of concrete that can negatively affect the compressive strength.

Therefore, petrographic examinations and air-void analyses of concrete in the core showed high air content i.e. higher-than the reported maximum air content of 7.5 percent to be the reason for reported lower-than-design compressive strength of concrete. Every one percent point increase in air from the design air content, at a given workability, can reduce the compressive strength by 3 to 5 percent. The overall fly ash content in the cylinder is found to be as per the reported proportion in the mix design. The estimated total cementitious materials content is also within the reported design limit. The overall water-cementitious materials ratio, a pivotal parameter to control compressive strength of concrete, is also found to be reasonable in the cylinder and not higher than the design value of 0.45 to affect the strength. There is no evidence of restricted Portland cement hydration or any unusual characteristics of cement hydration found in the microstructure of paste to interfere with the normal strength development. Therefore, other than the excessive air, no other evidence is found to cause the reported strength loss. A careful control of dosages of air entraining chemicals are needed to have a better control on the resultant air content of hardened concrete, and its compressive strength.

As a side comment, not related to the investigation of low strength but relevant to future durability of concrete in a moist outdoor environment of cyclic freezing and thawing is the potential unsoundness of crushed greywacke coarse aggregate particles and argillaceous component of fine aggregate particles seen in this concrete, which are known to cause pop out-type distress on concrete slab surface when exposed to moisture and freezing at critically saturated conditions. For long-term durability and serviceability, it is beneficial to replace these #57 crushed greywacke coarse aggregate particles by crushed limestone particles and removing (or reducing) the argillaceous (shale, siltstone) component in sand.

INTRODUCTION

Reported herein are the results of detailed laboratory studies of a hardened concrete cylinder previously tested for compressive strength to investigate reported lower-than-design compressive strength of concrete.

BACKGROUND INFORMATION

The reported mix design (PennDOT AAA mix) contains (in a cubic yard):

- 600 pounds of ASTM C 150 Type II Portland cement,
- 150 pounds of ASTM C 618 Class F fly ash (20 percent fly ash by weight of total cementitious materials),
- 1678 pounds of #57 crushed stone coarse aggregate,
- 1094 pounds of sand,
- 337 pounds of water,
- Sika Plastocrete 250 @ 5 oz/cwt of total cementitious materials,
- Sika Viscocrete 1000 @ 1 oz/cwt of total cementitious materials, and,
- Sika AEA @ 1 oz./cu. yd.

All above to comply with PennDOT AAA Mix design having a water-cementitious materials ratio of 0.45, a 28-day design strength of 4000 psi, and a design weight of 142.4 pounds per cubic yard. According to PennDOT Specification 704, the range of design air content is 3.5 to 7.5 percent.

PURPOSE OF PRESENT INVESTIGATION

Based on the background information provided, and concrete mix design provided, the purposes of the present investigation are to determine:

a. The composition, quality, and overall condition of concrete in the cylinder;
b. Evaluation of concrete materials and mix proportions to compare with the reported concrete mix; and,
c. Finally, based on detailed laboratory investigation, investigation of all possible reasons to explain the reported lower-than-anticipated compressive strength of concrete.

METHODOLOGIES

PETROGRAPHIC EXAMINATIONS (ASTM C 856)

The cylinder was examined by following the methods of ASTM C 856 "Standard Practice for Petrographic Examination of Hardened Concrete." Details of concrete petrography, and sample preparation techniques for petrographic examinations of concrete are provided in Jana (2006).

Briefly, the steps followed during petrographic examination of the cylinder include:

i. Visual examinations of the cylinder, as received, including adequate documentation of dimensions, measurements, condition, physical properties, integrity, etc.;
ii. Low-power stereo microscopical examinations of as-received, saw-cut and freshly fractured sections, and lapped circular section of cylinder for evaluation of textures, air-void system, and composition;
iii. Examinations of oil immersion mounts in a petrographic microscope for mineralogical compositions of specific areas of interests;

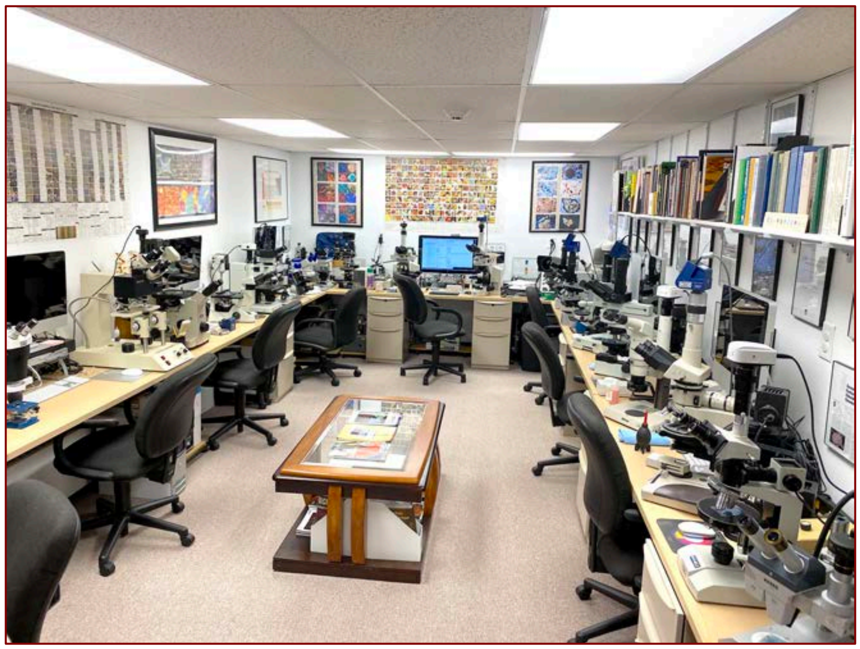

Figure 1: CMC's petrographic laboratory that houses various optical microscopes used in this study.

iv. Examinations of blue dye-mixed (to highlight open spaces, cracks, etc.) low-viscosity epoxy-impregnated large area (50 mm × 75 mm) thin section of concrete in a petrographic microscope for detailed compositional and microstructural analyses;
v. Photographing the cylinder, as received and at various stages of preparation with a digital camera and a flatbed scanner;
vi. Photomicrographs of lapped sections and thin section of cylinder taken with stereomicroscope and petrographic microscope, respectively to provide detailed compositional and mineralogical information of concrete; and,
vii. Various stereomicroscopes, petrographic microscopes (equipped with reflected, transmitted, polarized and fluorescent-light facilities), and digital cameras attached to those microscopes (see Figure 1) were used during this study. Micrographs from such examinations are provided in a series of Figures in this report.

AIR-VOID ANALYSIS (ASTM C 457)

Air-void analysis of concrete was done on the lapped circular section of cylinder by following the modified point count method procedure of ASTM C 457 "Standard Test Method for Microscopical Determination of Parameters of the Air-Void System in Hardened Concrete." Details of air-void analysis are described below.

a. A Velmex XY stage was used for point count. It was ensured that the total translation of the stage was at least 100 mm (4.0 in.) in each direction to cover a maximum area of 16 sq. in. It was also ensured that the intervals between the stops correspond to a translation of the stage a distance of 0.025 to 0.64 to 5.0 mm (0.025 to 0.200 in.). The magnitude of the average translation of the stage between stops was determined to the nearest 0.03 mm (0.001 in.). A total of five digital counters were used for calculating aggregates, paste, entrained and entrapped voids, and total voids intercepted during the traverse. A high-resolution stereomicroscope attached to a high-resolution and high frame rate digital microscope camera was used to capture live images of the lapped concrete surface on the PC screen during the traverses.

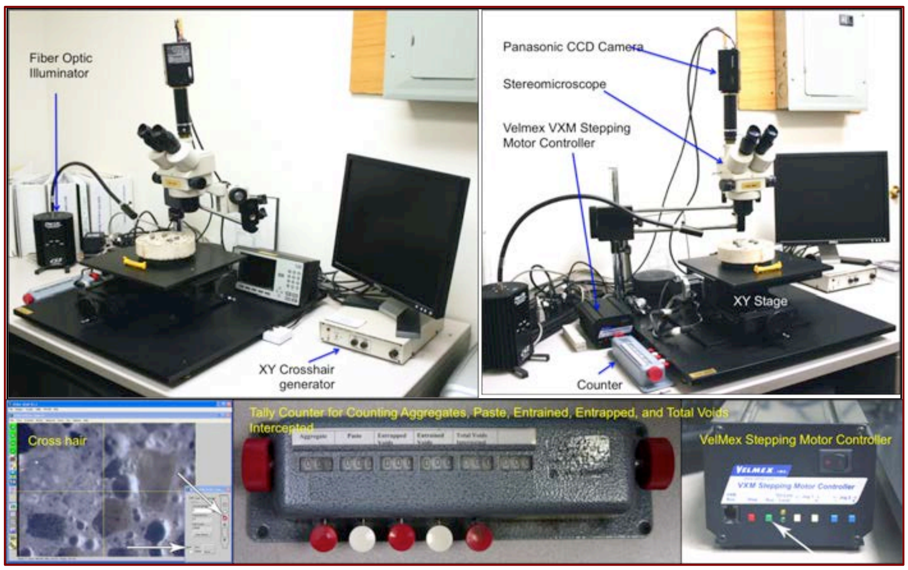

Figure 2: Set-up in the CMC laboratory for air-void analysis in hardened concrete by the modified point count method of ASTM C 457.

b. The lapped section of concrete was place on the stage and leveled with multiple spirit levels. Reflected light from the gooseneck of a fiber optic light source was incident upon the lapped surface at a low angle to highlight the air voids with their shadows. Superimposed in the computer screen was the index point of the cross hairs to pinpoint the area to be counted. A magnification not less than 50X was used and wasn't changed during the course of the analysis.

c. Minimum length of traverse and minimum number of points for the modified point count method are: (a) 2540 mm (100 in.) and 1500 points for $1^1/_2$-in. nominal size aggregate, (b) 2413 mm (95 in.) and 1425 points for 1-in. nominal size aggregate, (c) 2286 mm (90 in.) and 1350 points for $^3/_4$-in. nominal size aggregate, (d) 2032 mm (80 in.) and 1200 points for $^1/_2$-in. nominal size aggregate, and (e) 1905 mm (75 in.) and 1125 points for $^3/_8$-in. nominal size aggregate.

d. Air-void parameters were calculated by using the equations provided in C 457.

SAMPLE

PHOTOGRAPHS, IDENTIFICATION, INTEGRITY, AND DIMENSION

Figure 3 shows the broken, cracked previously strength-tested 6 in. × 12 in. concrete cylinder received for petrographic examinations.

END SURFACES

Due to consolidation in a cylinder mold for laboratory curing, one end of the cylinder has a smooth flat formed surface at the base and the top exposed end is finished. Both ends, however, are severely cracked and fragmented due to prior strength testing.

CRACKING & OTHER VISIBLE DISTRESS, IF ANY

Extensive macro and micro cracking are present from strength test, which are usual and not relevant to the present investigation of low strength.

EMBEDDED ITEM

There are no wire mesh, fibers, or other embedded items found in the cylinder.

RESONANCE

The cylinder has a ringing resonance, when hammered.

TESTING STRATEGY

To have a better integrity during sample processing for petrographic examinations, the cylinder was first wrapped with a 3M duct tape. A circular section was sectioned with a water-cooled diamond saw for subsequent lapping on a flat horizontal rotating iron lapping wheel with various metal and resin-bonded diamond abrasive discs using water as coolant. The lapped circular section was used for stereo microscopical examinations of concrete, examinations of air content and air-void system and eventual determination of air void parameters of concrete by modified point count method of ASTM C 457. Another section was made for preparation of a blue dye-mixed epoxy-impregnated thin section for examinations in a petrographic microscope.

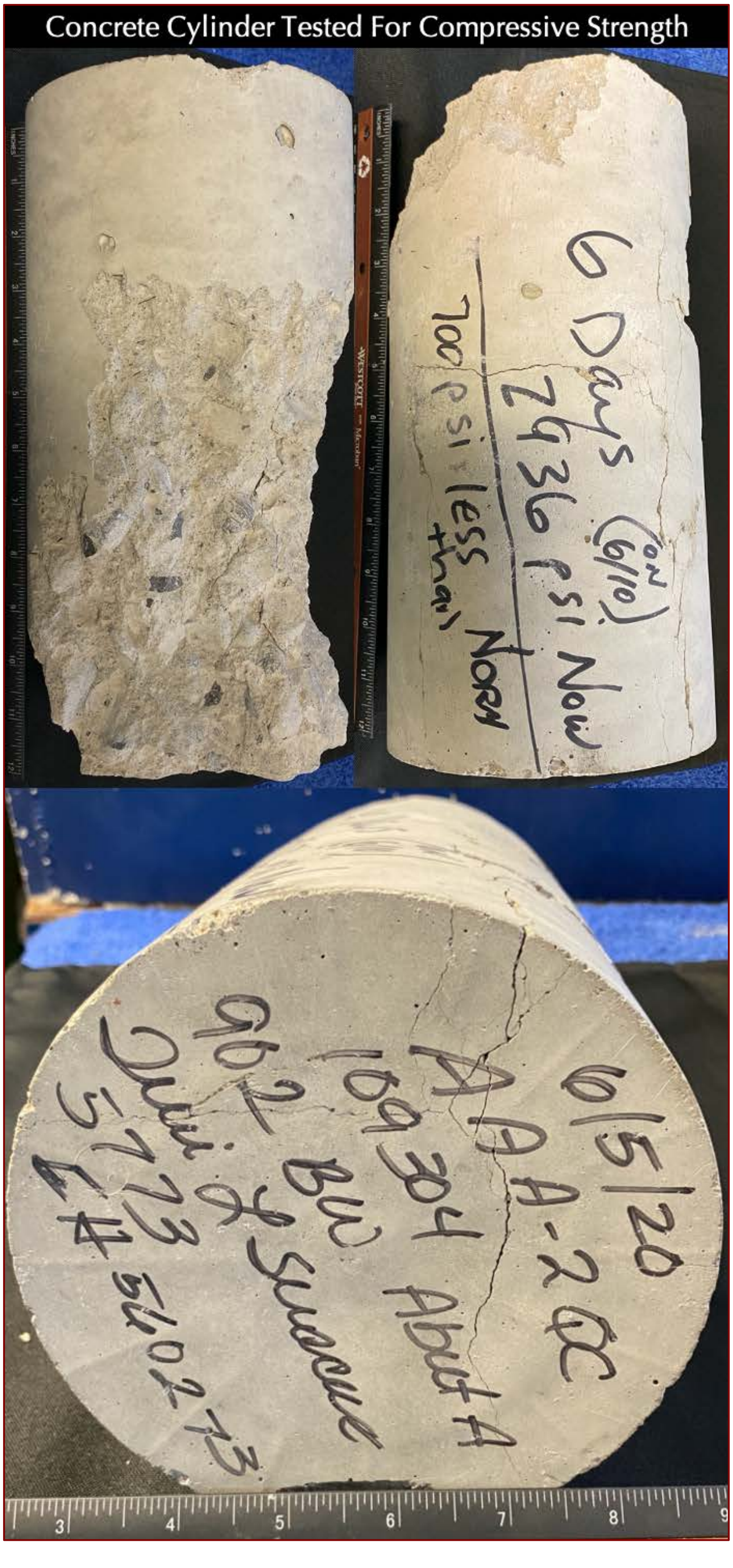

Figure 3: Shown is the previously strength-tested cracked, broken, fragment of a 6 in. × 12 in. size concrete cylinder with identification that was used for petrographic examinations.

PETROGRAPHIC EXAMINATIONS

LAPPED CIRCULAR SECTION

Figure 4: Lapped circular section of the cylinder showing: (a) cracks (many are marked in red) formed from strength testing, (b) dark, dense, hard crushed stone coarse aggregate particles which are determined to be greywacke (a sedimentary rock, a variety of sandstone containing detrital quart, feldspar grains in an argillaceous i.e., wacke-type matrix, (c) natural siliceous sand fine aggregate particles, (d) medium to dark gray interstitial paste, and (d) overall dense and well-consolidated nature of concrete due to good consolidation practice during preparation of cylinder in its mold.

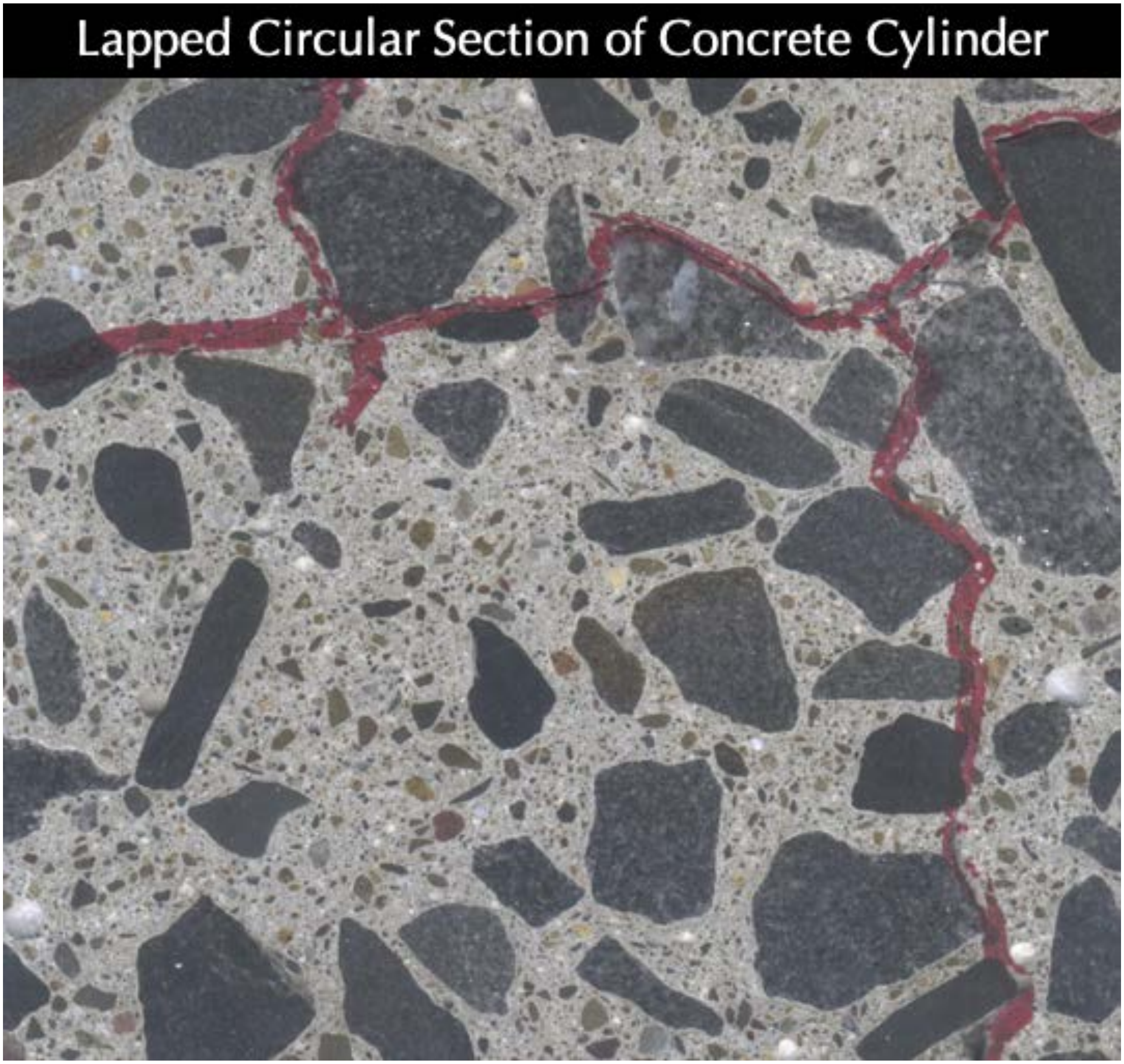

Figure 5: Enlarged view of the lapped section of concrete showing: (a) cracks (many are marked in red) formed from strength testing, (b) dark, dense, hard crushed stone coarse aggregate particles which are determined to be greywacke (a sedimentary rock, a variety of sandstone containing detrital quart, feldspar grains in an argillaceous i.e., wacke-type matrix, (c) natural siliceous sand fine aggregate particles, (d) medium to dark gray interstitial paste, and (d) overall dense and well-consolidated nature of concrete due to good consolidation practice during preparation of cylinder in its mold.

MICROGRAPHS OF LAPPED CIRCULAR SECTION

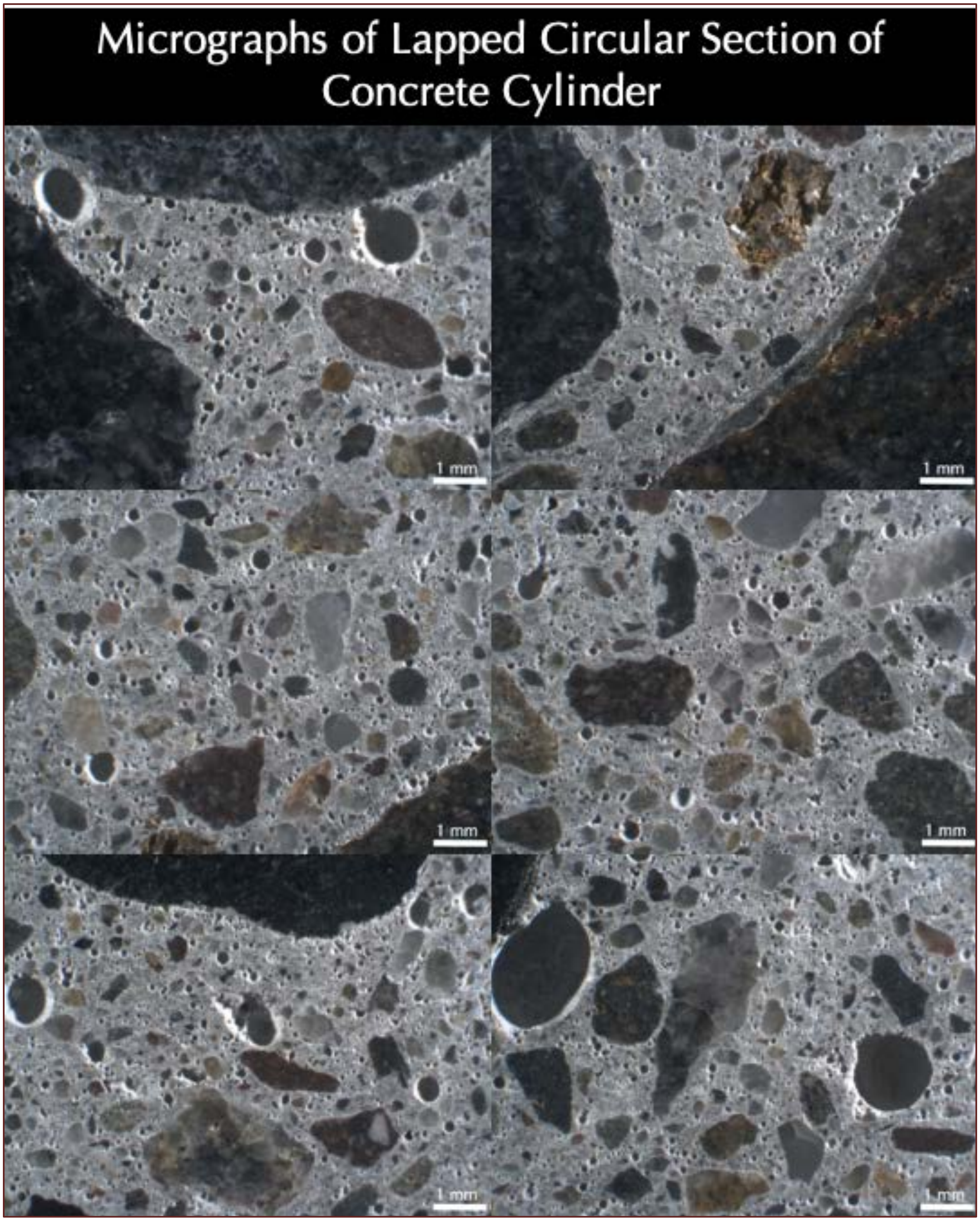

Figure 6: Mosaic of six micrographs of lapped circular section of cylinder taken with a stereo-microscope showing: (a) numerous fine, discrete, spherical and near-spherical entrained air voids of sizes 1 mm or less; (b) a few coarse, near-spherical and irregular-shaped entrapped air voids that were formed during consolidation of cylinder in the mold; (c) excessive air entrainment in concrete having too many fine air bubbles; (d) a dark rim of paste along some margins of crushed greywacke coarse aggregate particles due to absorption of some mix water by the absorptive greywacke particles (one such dark paste rim is seen in the top right photo along the margin of right stone particle).

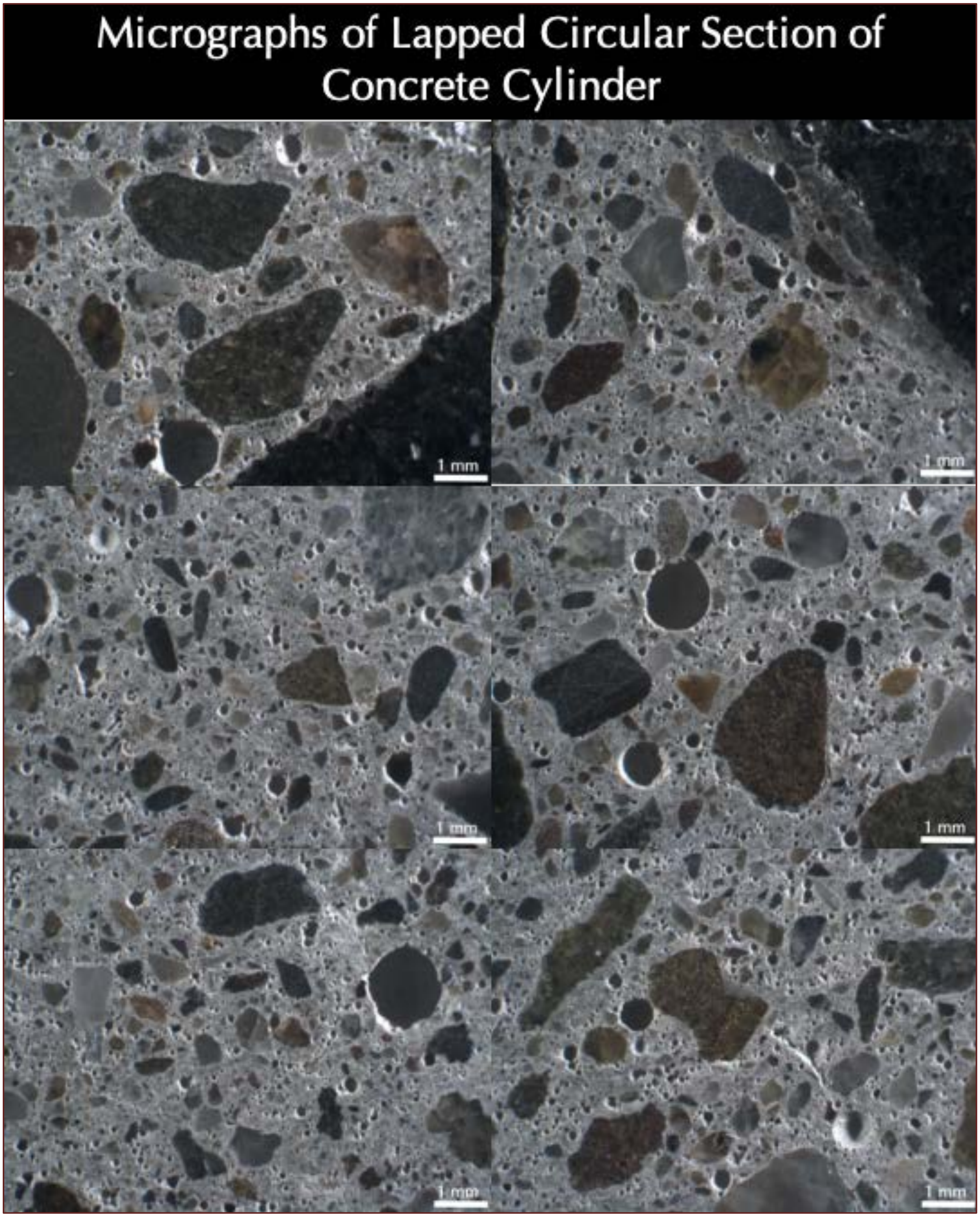

Figure 7: Mosaic of six micrographs of lapped circular section of cylinder taken with a stereo-microscope showing: (a) numerous fine, discrete, spherical and near-spherical entrained air voids of sizes 1 mm or less; (b) a few coarse, near-spherical and irregular-shaped entrapped air voids that were formed during consolidation of cylinder in the mold; (c) excessive air entrainment in concrete having too many fine air bubbles; (d) a dark rim of paste along some margins of crushed greywacke coarse aggregate particles due to absorption of some mix water by the absorptive greywacke particles (one such dark paste rim is seen in the top right photo along the margin of right stone particle).

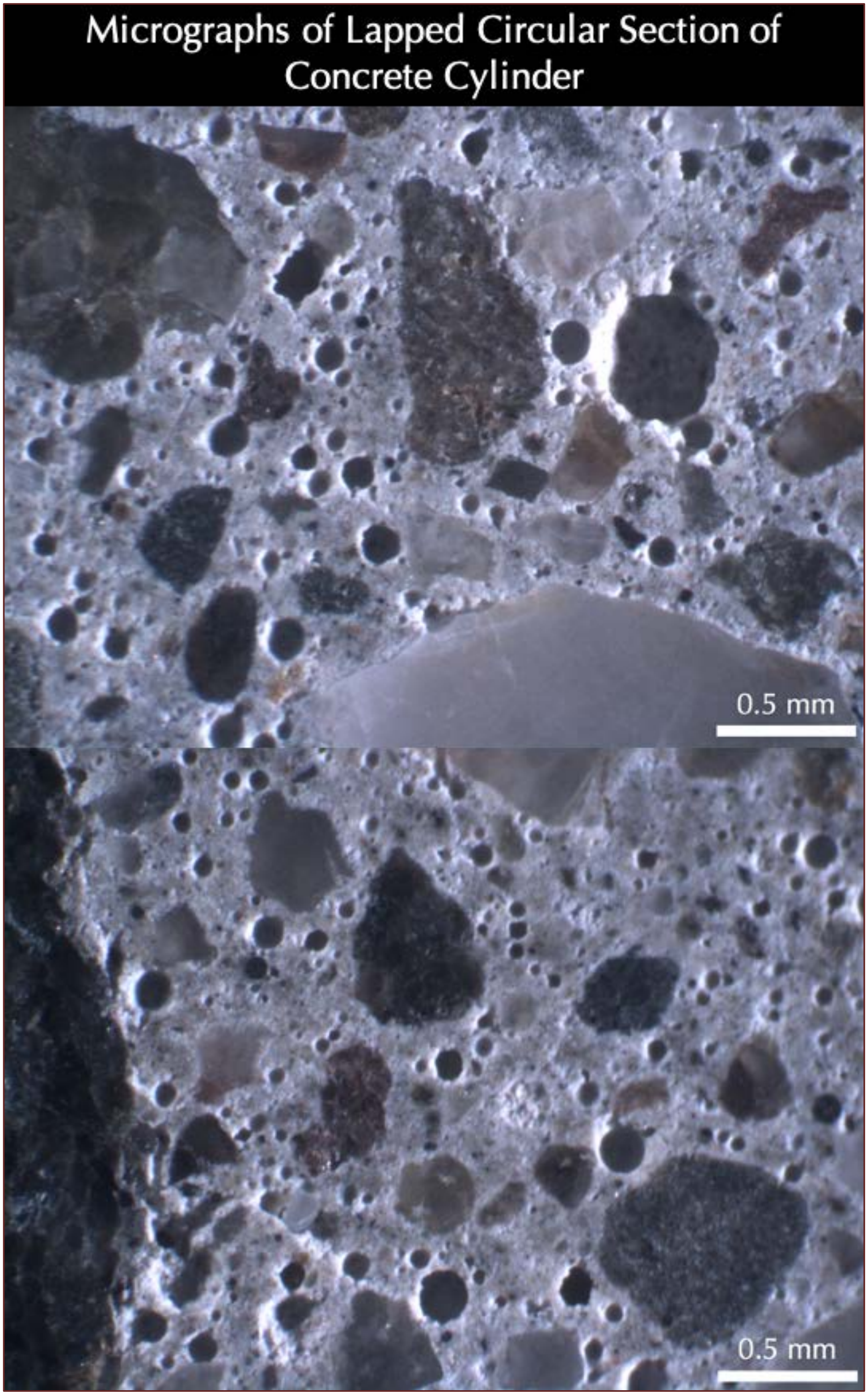

Figure 8: Two micrographs of lapped section of concrete showing abundant fine spherical entrained air bubbles in concrete.

The concrete is air entrained as shown by such distribution of fine spherical entrained air bubbles. However, the overall air content appeared to be at the high end of the reported air content range of 3.5 to 7.5 percent which has required further investigation of this concrete by modified point count method of ASTM C 457.

The total air content is determined to be 8.12 percent.

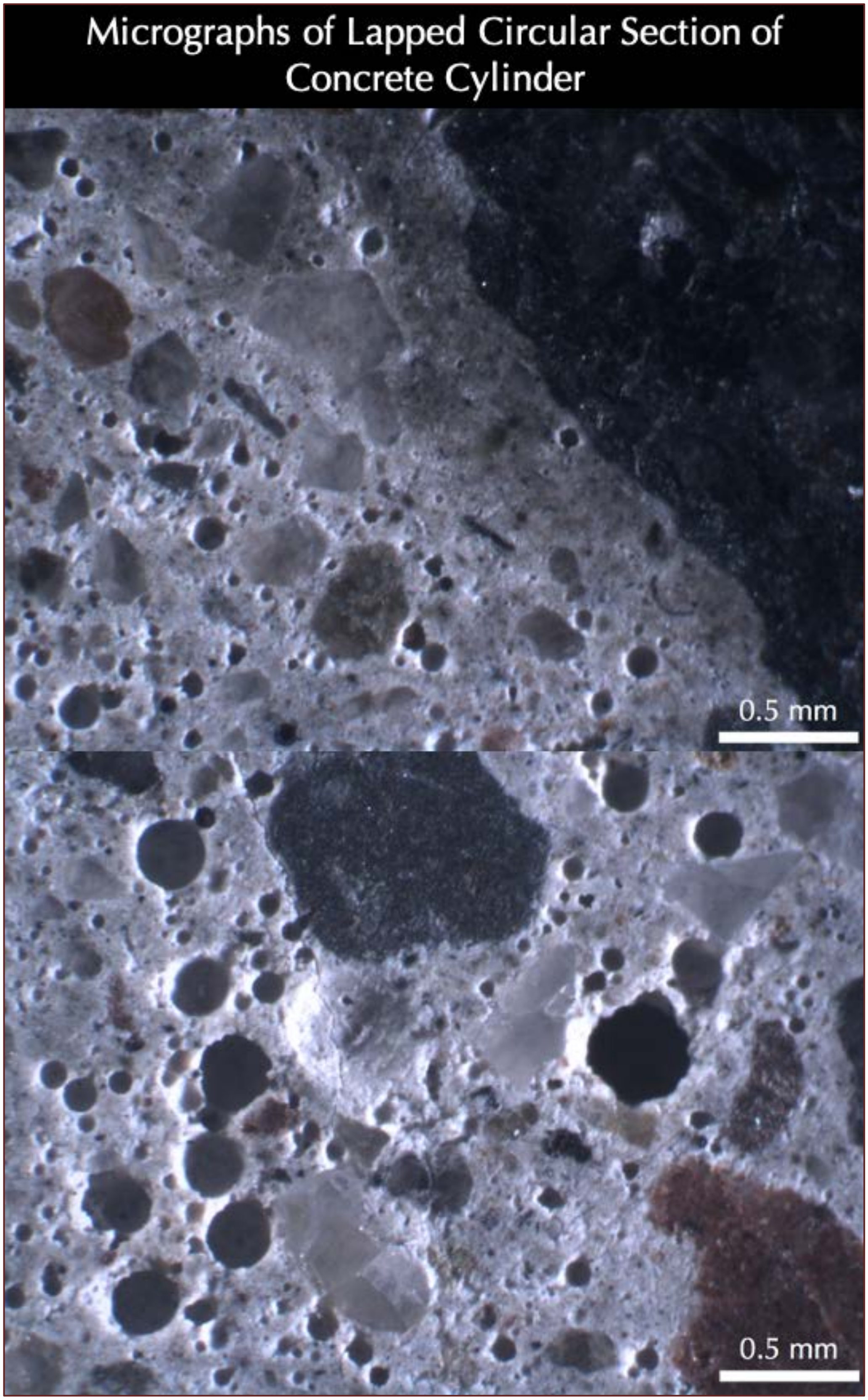

Figure 9: Two micrographs of lapped section of concrete showing: (a) abundant fine spherical entrained air bubbles in concrete, and (b) a rim of dark paste along the margin of a crushed graywacke coarse aggregate particle in the top photo due to absorption of some mix water by the absorptive greywacke particle.

The argillaceous, i.e. wacke-type matrix of greywacke absorb some mix water to create the dark paste rim.

Such absorption of particle can also potentially cause pop-out distress when these aggregate particles are present near the finished surface of slab and get saturated with moisture during service (or exposed to freezing at moisture-saturated condition).

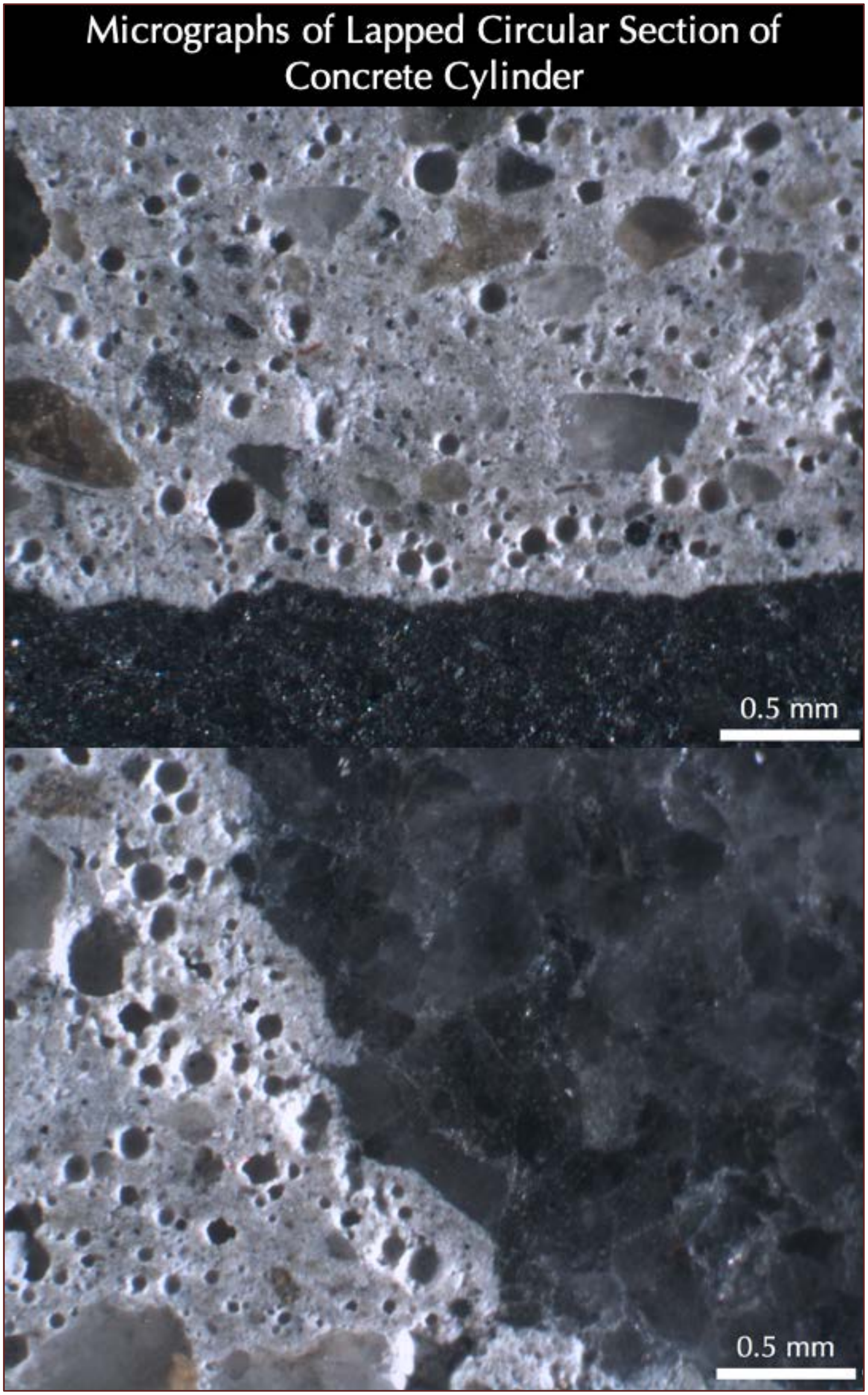

Figure 10: Two micrographs of lapped section of concrete showing: (a) abundant fine spherical entrained air bubbles in concrete, and (b) clustering of air voids along the interface between a crushed stone coarse aggregate particle and the mortar fraction of concrete in the bottom photo.

Such void clustering along aggregate-paste interface can weaken the aggregate-paste bond, and, thereby, reduces the compressive strength of concrete.

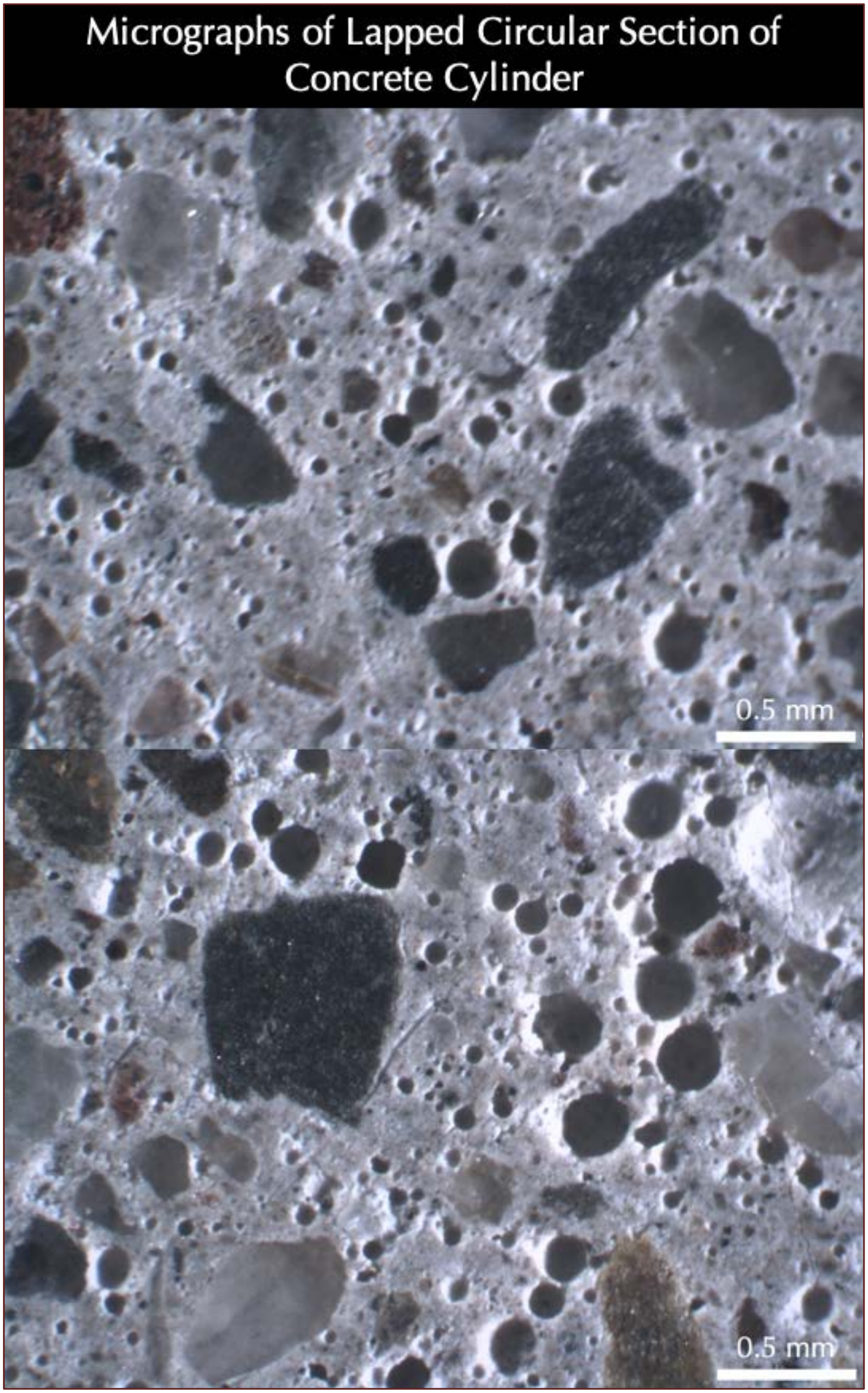

Figure 11: Further micrographs of lapped section of concrete showing excessive air entrainment and distribution of fine spherical entrained air bubbles across the paste.

Such bubbles are necessary for freeze-thaw durability of concrete. However, uncontrolled dosage of air entraining chemical to generate more than necessary bubbles can reduce the compressive strength of concrete (Jana et al. 2005).

THIN SECTION

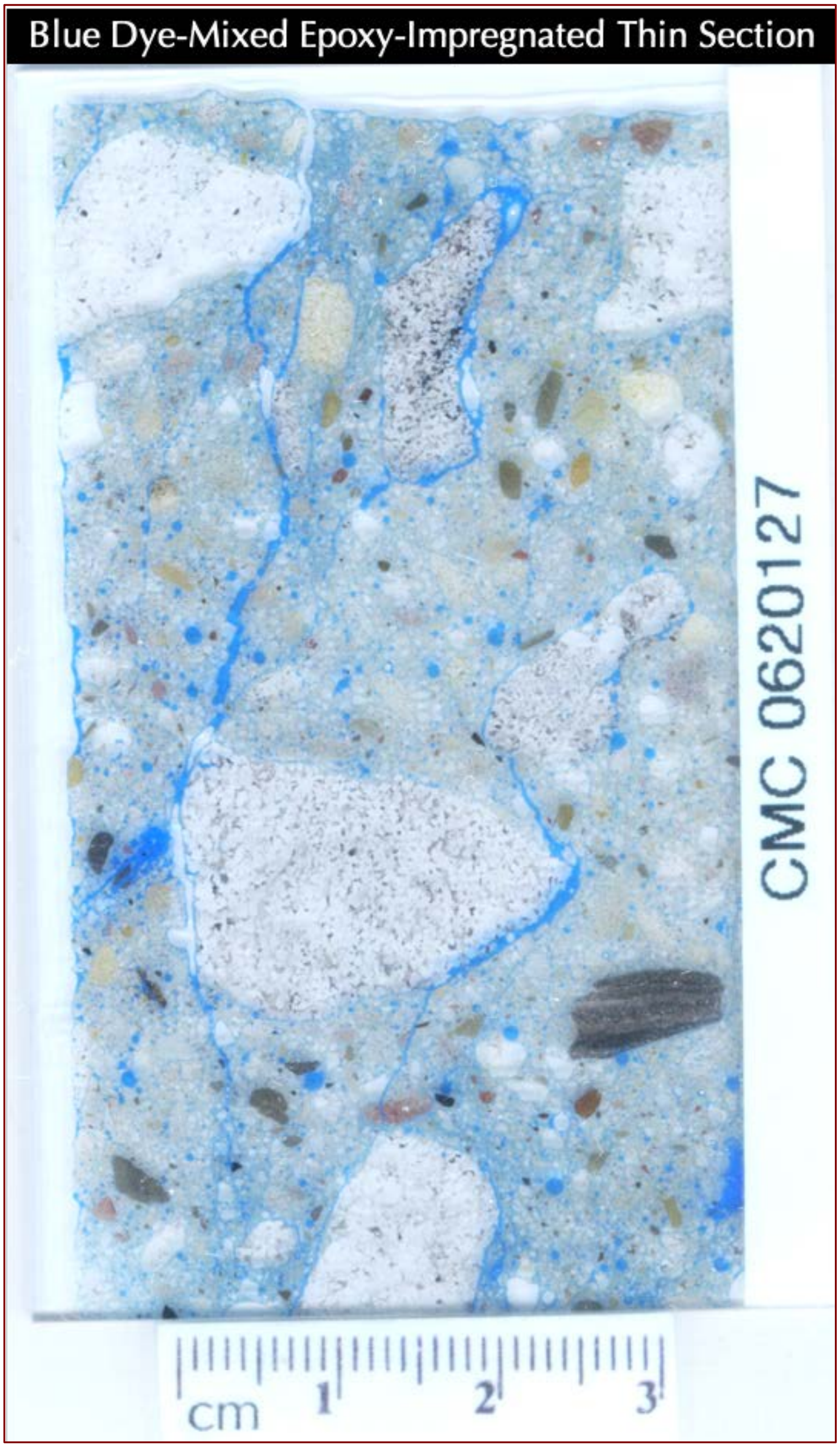

Figure 12: Blue dye-mixed epoxy-impregnated thin section of concrete showing cracks from previous strength test and air voids that are highlighted by the blue epoxy.

Notice crushed greywacke coarse aggregate particles, natural siliceous sand fine aggregate particles and entrained air void distribution in the thin section.

MICROGRAPHS OF THIN SECTION

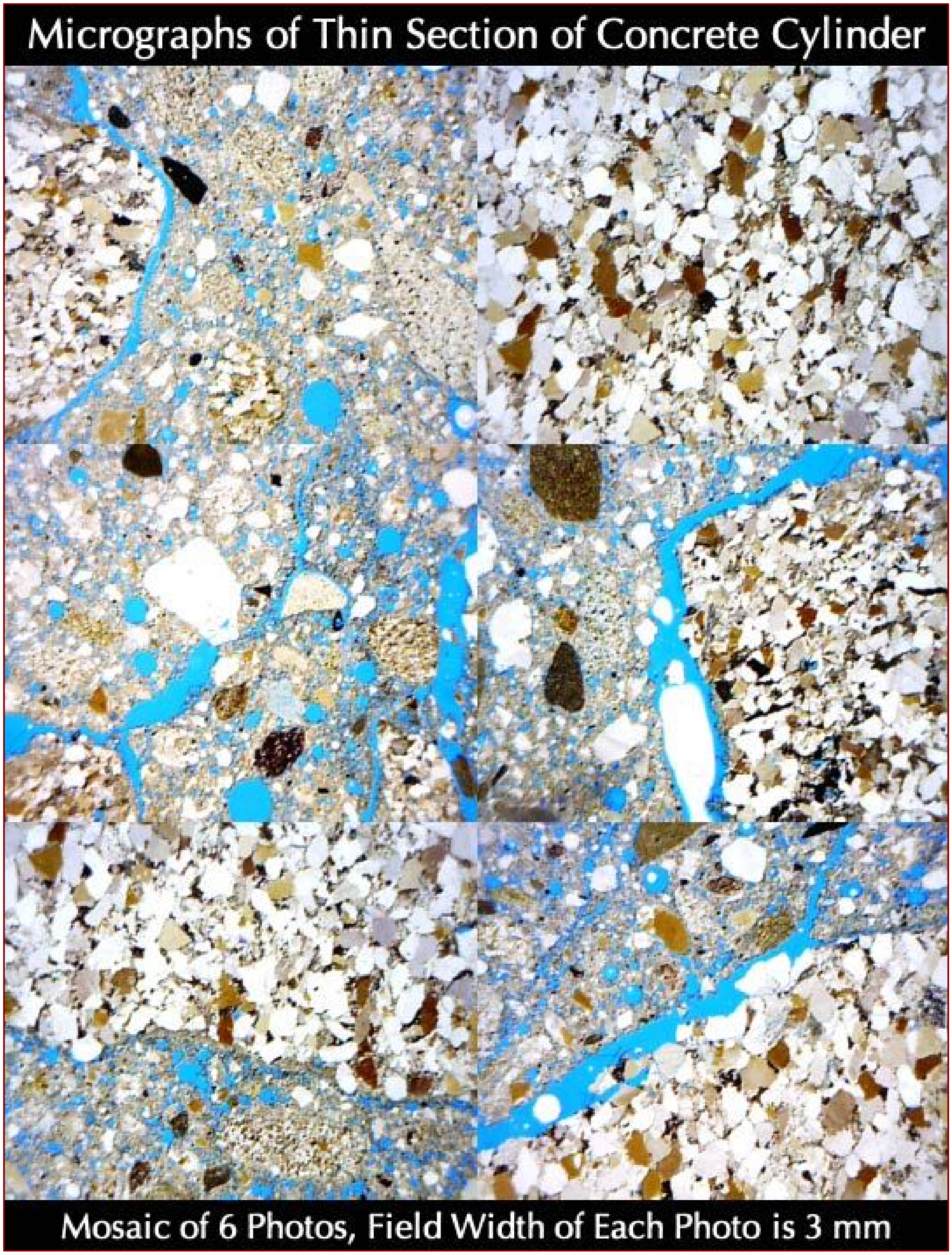

Figure 13: Micrographs of blue dye-mixed epoxy-impregnated thin section of concrete showing: (a) crushed greywacke coarse aggregate particles consisting of detrital quartz and feldspar grains in an argillaceous (wacke-type) matrix; (b siliceous-argillaceous sand fine aggregate particles consisting of major amounts of quartz, quartzite, feldspar and subordinate amounts of shale and siltstone particles; (c) entrained air voids highlighted by blue epoxy; and (d) cracks formed from strength testing, which are also highlighted by blue epoxy.

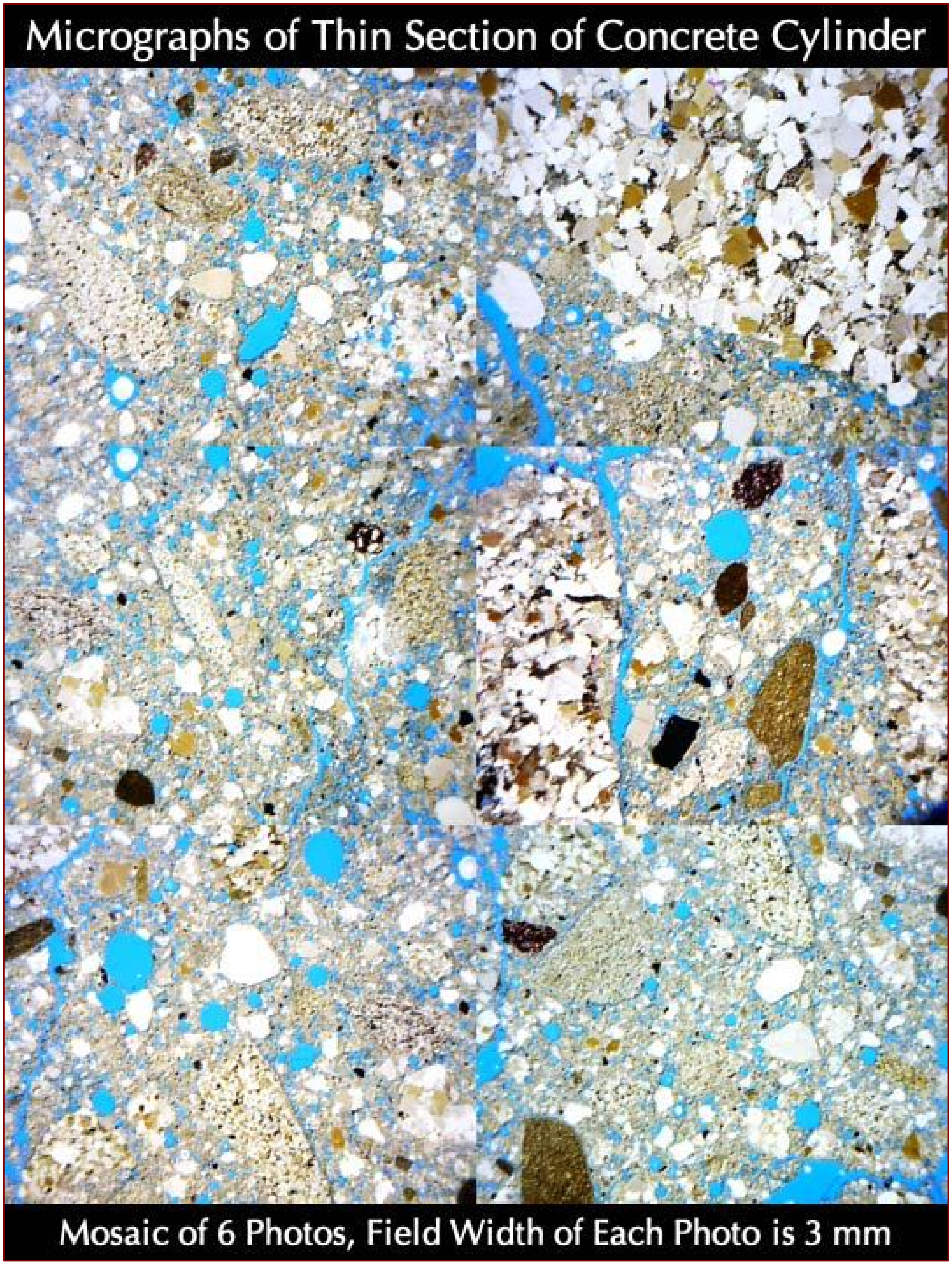

Figure 14: Micrographs of blue dye-mixed epoxy-impregnated thin section of concrete showing: (a) crushed greywacke coarse aggregate particles consisting of detrital quartz and feldspar grains in an argillaceous (wacke-type) matrix; (b) siliceous-argillaceous sand fine aggregate particles consisting of major amounts of quartz, quartzite, feldspar and subordinate amounts of shale and siltstone particles; (c) entrained air voids highlighted by blue epoxy; and (d) cracks formed from strength testing, which are also highlighted by blue epoxy.

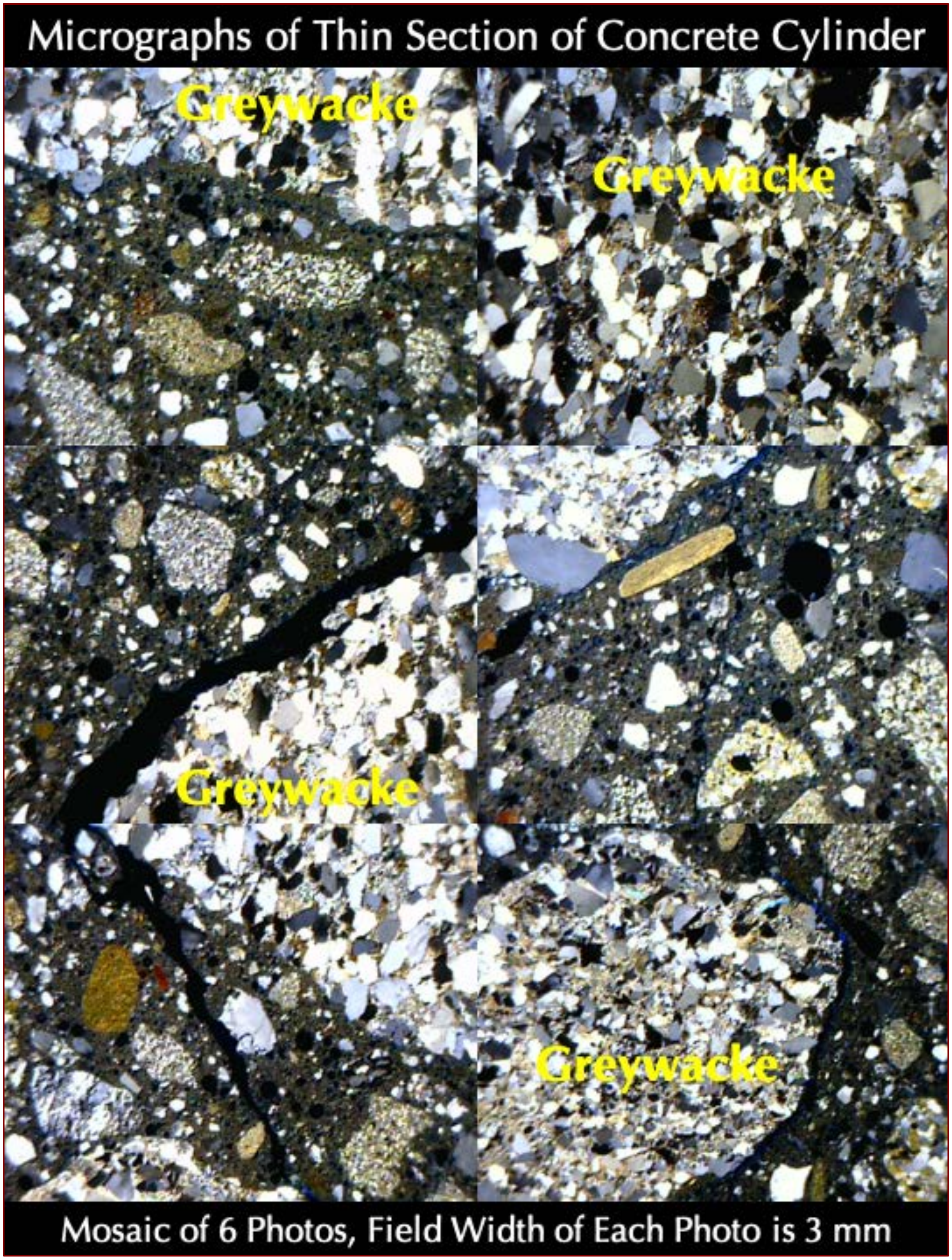

Figure 15: Micrographs of blue dye-mixed epoxy-impregnated thin section of concrete showing: (a) crushed greywacke coarse aggregate particles consisting of detrital quartz and feldspar grains in an argillaceous (wacke-type) matrix; and (b) siliceous-argillaceous sand fine aggregate particles consisting of major amounts of quartz, quartzite, chert, feldspar and subordinate amounts of shale and siltstone particles. Photos were taken in crossed polarized light mode with a transmitted-light high-power stereo-zoom microscope.

Figure 16: Micrographs of blue dye-mixed epoxy-impregnated thin section of concrete showing: (a) crushed greywacke coarse aggregate particles consisting of detrital quartz and feldspar grains in an argillaceous (wacke-type) matrix; and (b) siliceous-argillaceous sand fine aggregate particles consisting of major amounts of quartz, quartzite, chert, feldspar and subordinate amounts of shale and siltstone particles. Photos were taken in crossed polarized light mode with a transmitted-light high-power stereo-zoom microscope.

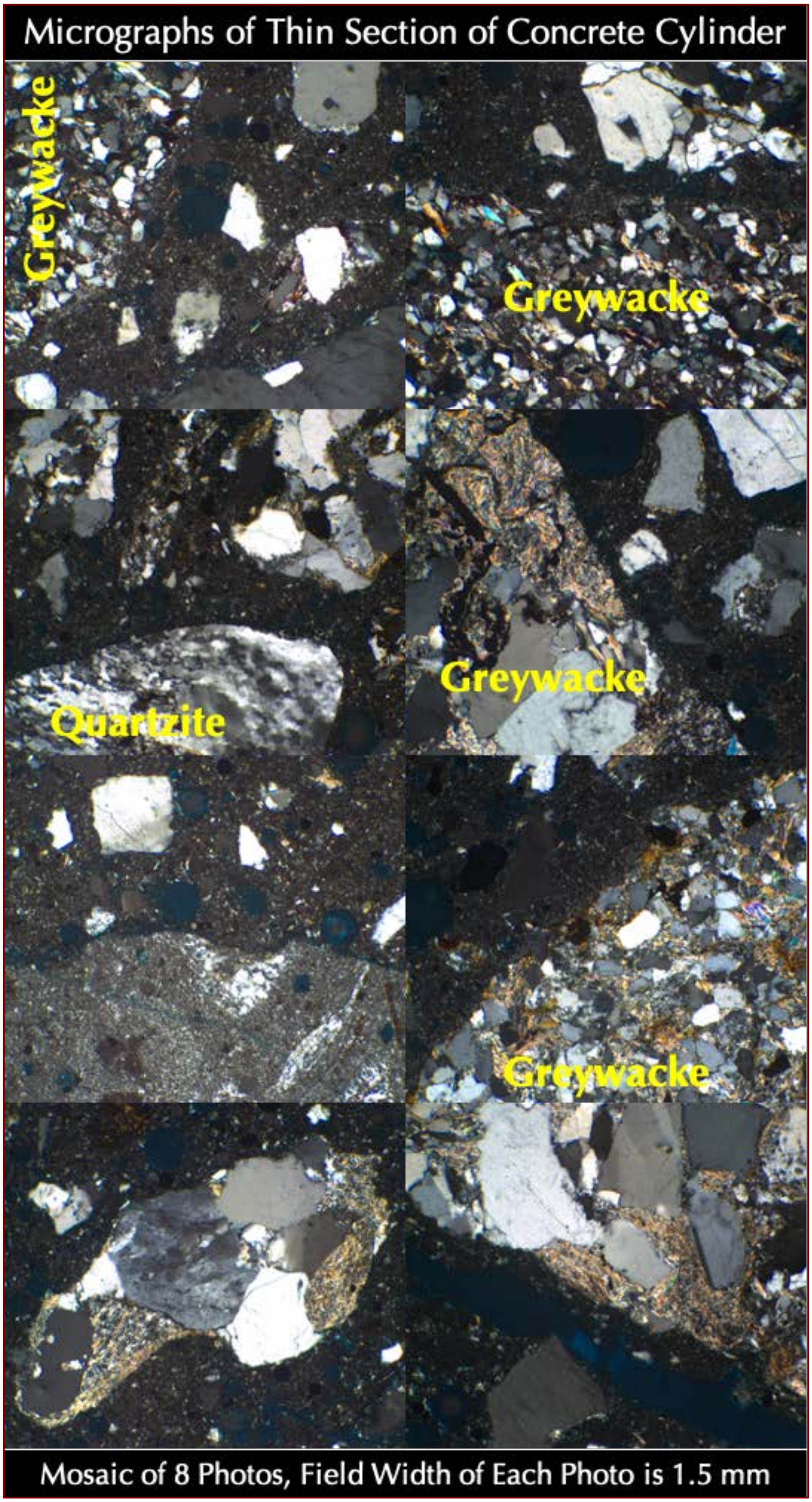

Figure 17: Micrographs of blue dye-mixed epoxy-impregnated thin section of concrete showing: (a) crushed greywacke coarse aggregate particles consisting of detrital quartz and feldspar grains in an argillaceous (wacke-type) matrix; and (b) siliceous-argillaceous sand fine aggregate particles consisting of major amounts of quartz, quartzite, chert, feldspar and subordinate amounts of shale and siltstone particles. Photos were taken in crossed polarized light mode with a transmitted-light high-power stereo-zoom microscope.

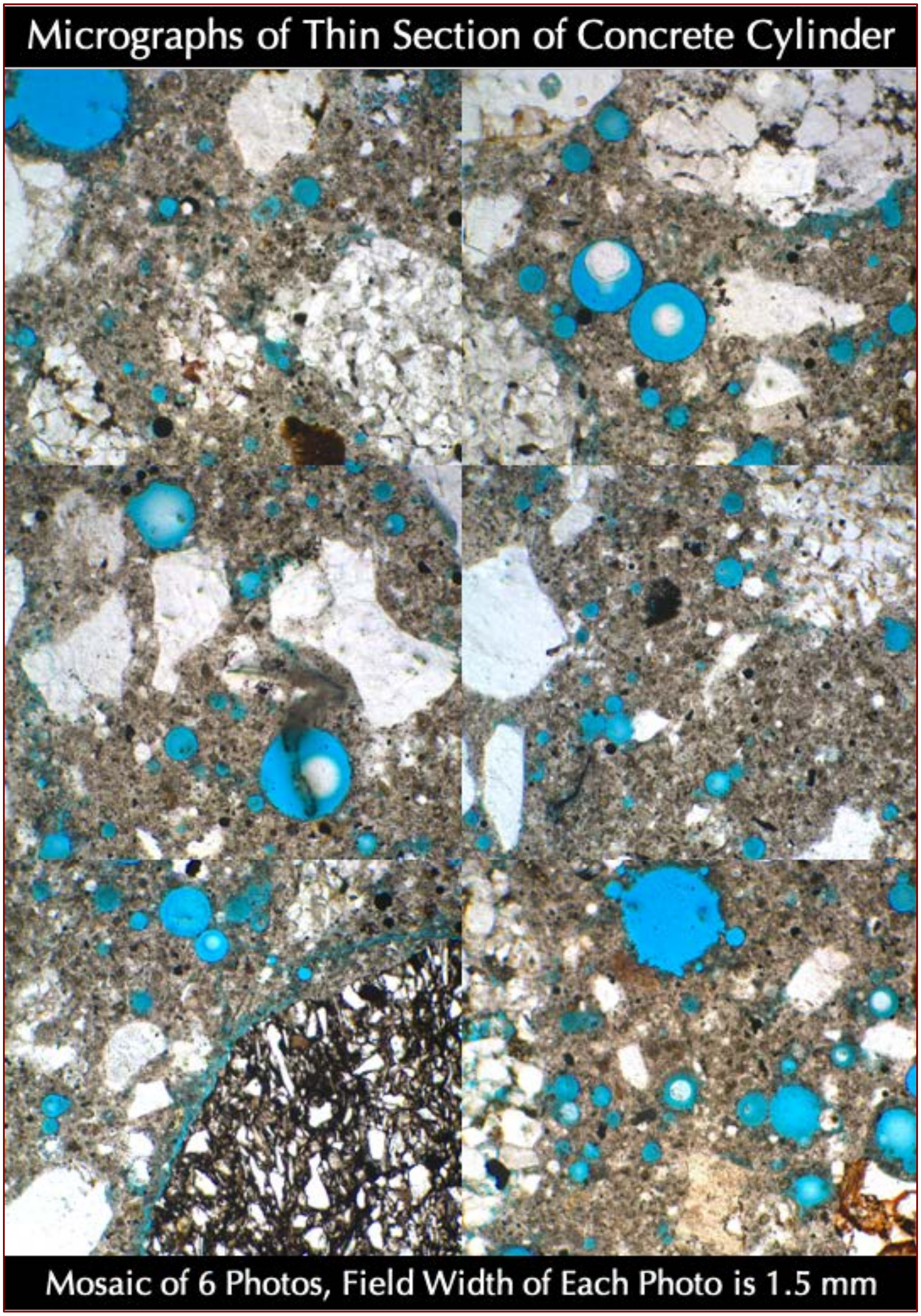

Figure 18: Micrographs of blue dye-mixed epoxy-impregnated thin section of concrete showing: (a) fine, spherical entrained air bubbles of sizes 1 mm or less that are highlighted by blue epoxy; (b) crushed greywacke coarse aggregate particles consisting of detrital quartz and feldspar grains in an argillaceous (wacke-type) matrix; and (c) siliceous-argillaceous sand fine aggregate particles consisting of major amounts of quartz, quartzite, chert, feldspar and subordinate amounts of shale and siltstone particles. Photos were taken in plane polarized light mode with a transmitted-light high-power fluorescent-light microscope.

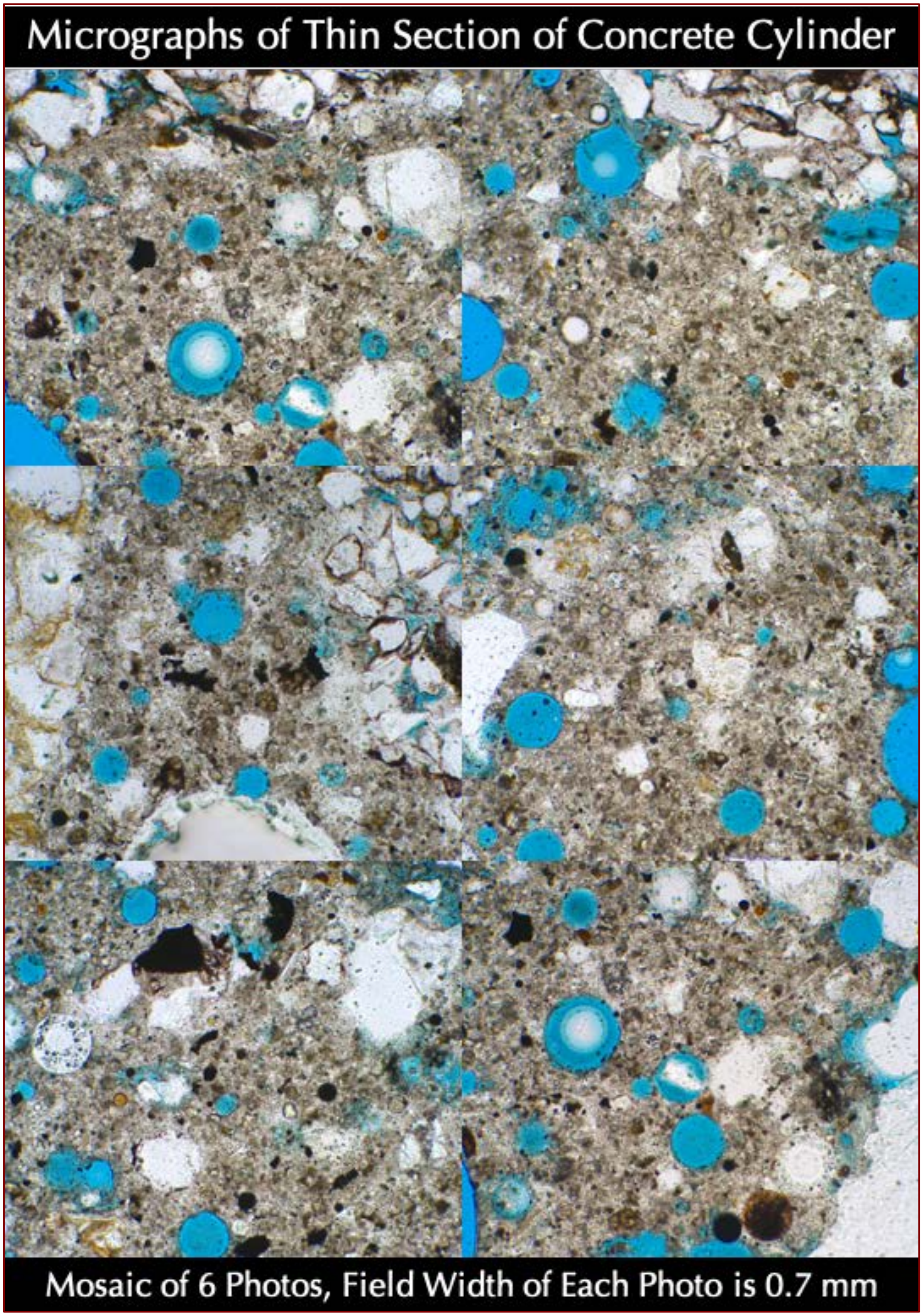

Figure 19: Micrographs of blue dye-mixed epoxy-impregnated thin section of concrete showing: (a) fine, spherical entrained air bubbles of sizes 1 mm or less that are highlighted by blue epoxy; (b) crushed greywacke coarse aggregate particles consisting of detrital quartz and feldspar grains in an argillaceous (wacke-type) matrix; and (c) siliceous-argillaceous sand fine aggregate particles consisting of major amounts of quartz, quartzite, chert, feldspar and subordinate amounts of shale and siltstone particles. Photos were taken in plane polarized light mode with a transmitted-light high-power fluorescent-light microscope.

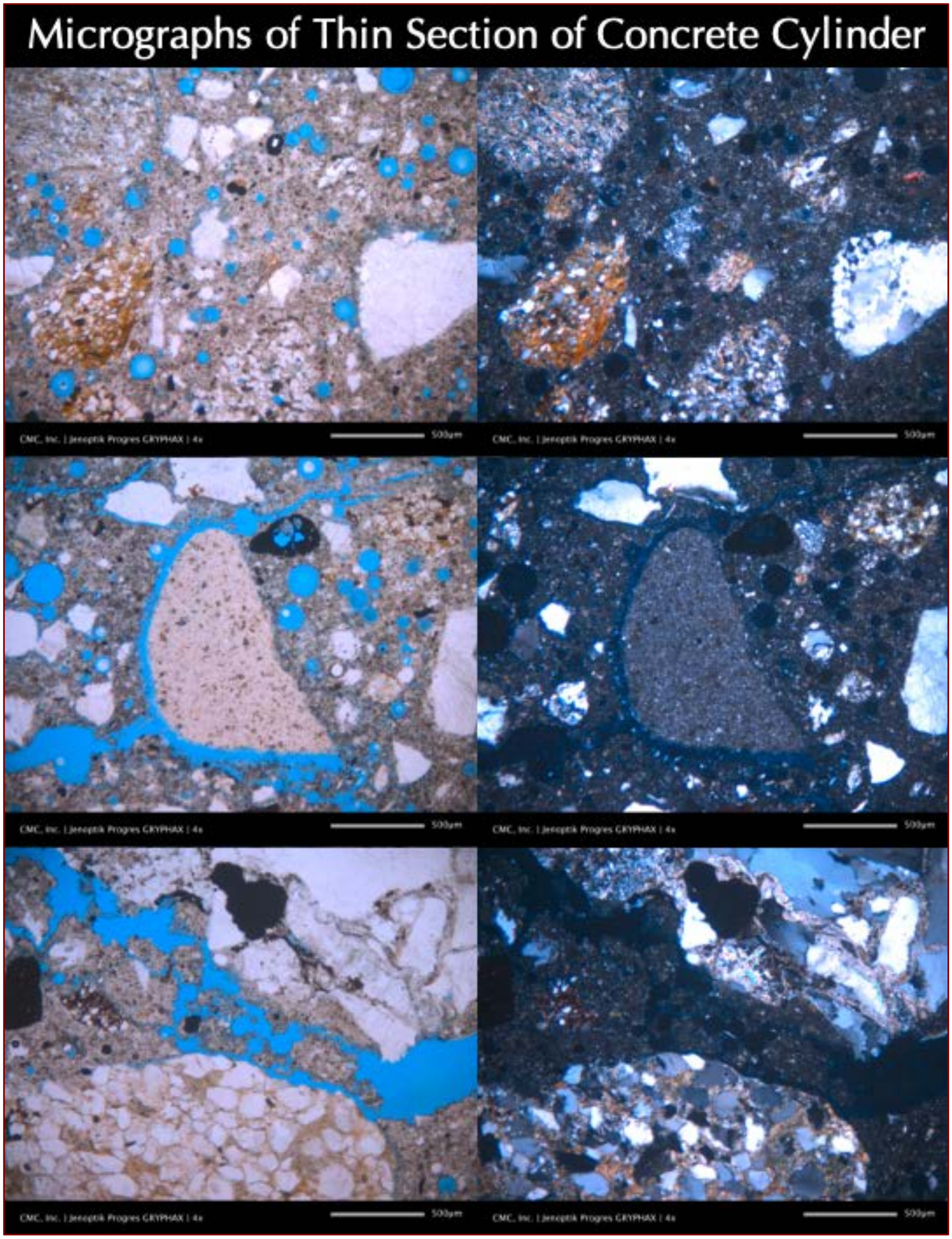

Figure 20: Micrographs of blue dye-mixed epoxy-impregnated thin section of concrete showing: (a) fine, spherical entrained air bubbles of sizes 1 mm or less that are highlighted by blue epoxy; (b) crushed greywacke coarse aggregate particles consisting of detrital quartz and feldspar grains in an argillaceous (wacke-type) matrix; and (c) siliceous-argillaceous sand fine aggregate particles consisting of major amounts of quartz, quartzite, chert, feldspar and subordinate amounts of shale and siltstone particles. Photos were taken in plane polarized light mode in left column and corresponding crossed polarized light mode in right column with a petrographic microscope.

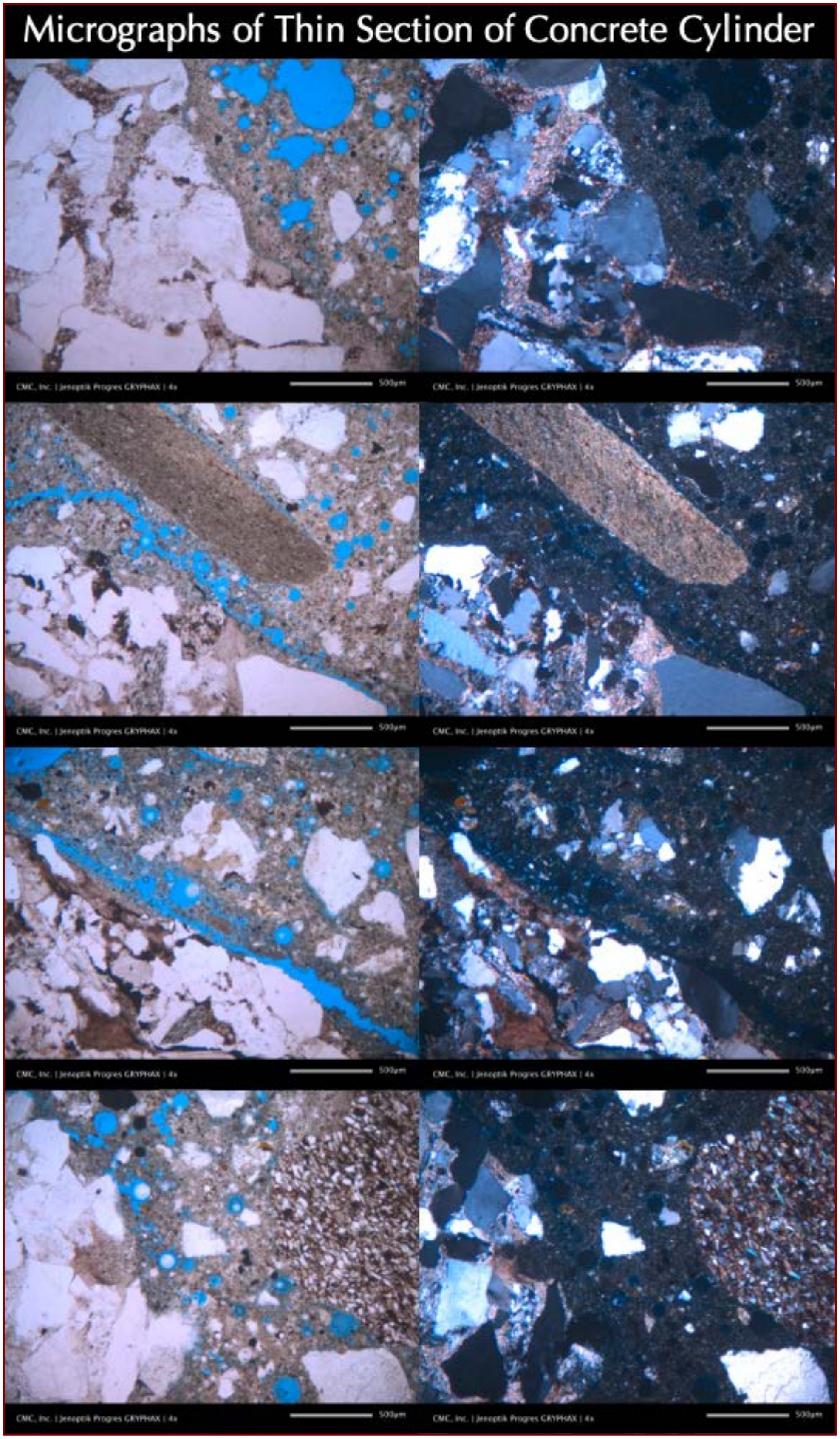

Figure 21: Micrographs of blue dye-mixed epoxy-impregnated thin section of concrete showing: (a) fine, spherical entrained air bubbles of sizes 1 mm or less that are highlighted by blue epoxy; (b) crushed greywacke coarse aggregate particles consisting of detrital quartz and feldspar grains in an argillaceous (wacke-type) matrix; and (c) siliceous-argillaceous sand fine aggregate particles consisting of major amounts of quartz, quartzite, chert, feldspar and subordinate amounts of shale and siltstone particles. Photos were taken in plane polarized light mode in left column and corresponding crossed polarized light mode in right column with a petrographic microscope.

COARSE AGGREGATE

Coarse aggregate is crushed greywacke (Figures 4 to 17) having a nominal maximum size of 1 in. (25 mm). Particles are angular, dense, hard, dark gray sedimentary rocks consisting of detrital quartz, feldspar and lithic (rock) fragments distributed in an argillaceous sericitic clay (wacke-type) matrix. Particles are equidimensional to elongated, unaltered, uncoated, and mostly uncracked except the ones along the crack paths formed during strength testing. Coarse aggregate particles are well-graded and well-distributed (Figure 4).

The greywacke particles are potentially unsound when exposed to moisture and freezing at critically saturated conditions. The argillaceous (wacke) matrix of greywacke can absorb moisture and cause expansion during critically saturated condition or if exposed to freezing. There is no evidence of alkali-aggregate reactions of coarse aggregate particles in the concrete. Coarse aggregate particles are judged not to have contributed to the reported lower-than-design compressive strength of concrete.

FINE AGGREGATE

Fine aggregate is natural siliceous-argillaceous sand (Figures 4 to 21) having a nominal maximum size of $^{3}/_{8}$ in. (9.5 mm). Particles contain major amounts of quartz, quartzite, feldspar, and subordinate amounts of chert, shale, and siltstone particles, and minor amounts of ferruginous rocks, and mafic minerals. Particles are variably colored, subangular to subrounded, dense, hard, equidimensional to elongated, unaltered, uncoated, and uncracked. Fine aggregate particles are well-graded and well-distributed. There is no evidence of alkali-aggregate reactions of fine aggregate particles in the concrete. Fine aggregate particles have been sound during their service. The argillaceous components (shale, siltstone) in fine aggregate are potentially unsound when exposed to moisture and freezing during service.

Table 1 summarizes properties of coarse and fine aggregates determined from the cylinder.

Properties and Compositions of Aggregates	Concrete Cylinder
Coarse Aggregate	
Types	Crushed Greywacke
Nominal maximum size	1 in. (25 mm)
Rock Types	Greywacke
Angularity, Density, Hardness, Color, Texture, Sphericity	Angular, dense, hard, dark gray sedimentary rocks consisting of detrital quartz, feldspar and lithic (rock) fragments distributed in an argillaceous sericitic clay (wacke-type) matrix. Particles are equidimensional to elongated,
Cracking, Alteration, Coating	Unaltered, uncoated, and mostly uncracked except the ones along the crack paths formed during strength testing
Grading & Distribution	Well-graded, Well-distributed
Soundness	Potentially unsound when exposed to moisture and freezing at critically saturated conditions

Properties and Compositions of Aggregates	Concrete Cylinder
Alkali-Aggregate Reactivity	None
Fine Aggregate	
Types	Natural siliceous-argillaceous sand
Nominal maximum size	$^3/_8$ in. (9.5 mm)
Rock Types	Major amounts of quartz, quartzite, feldspar, and subordinate amounts of chert, shale, and siltstone particles, and minor amounts of ferruginous rocks, and mafic minerals
Cracking, Alteration, Coating	Variably colored, subangular to subrounded, dense, hard, equidimensional to elongated, unaltered, uncoated, and uncracked
Grading & Distribution	Well-graded and Well-distributed
Soundness	Sound
Alkali-Aggregate Reactivity	The argillaceous components (shale, siltstone) in fine aggregate are potentially unsound when exposed to moisture and freezing during service

Table 1: Properties of coarse and fine aggregates of concrete in the cylinder.

PASTE

Properties and composition of hardened cement paste are summarized in Table 2. Paste is medium gray, dense, and hard. Freshly fractured surfaces have subvitreous lusters and subconchoidal textures. Residual and relict Portland cement particles are present and estimated to constitute 10 to 12 percent of the paste volume. Hydration of Portland cement is normal. Distributed throughout the paste are fine, spherical clear to light to dark brown to black glassy particles of fly ash having the fineness of Portland cement.

The textural and compositional features of the paste are indicative of a total cementitious materials content estimated to be equivalent to $7^1/_2$ to 8 bags of Portland cement per cubic yard, of which 20 percent is estimated to be fly ash. The water-cementitious materials ratio of paste is estimated to be 0.45.

There is no evidence of any deleterious secondary deposits found in the concrete. Bonds between the coarse aggregate particles and mortar fractions of concrete are moderately tight to weak at locations where clustering of air voids have occurred along the interfaces.

Properties and Compositions of Paste	Concrete Cylinder
Color, Hardness, Porosity, Luster	Medium gray, dense, and hard. Freshly fractured surfaces have subvitreous lusters and subconchoidal textures.
Residual Portland Cement Particles	10 to 12 percent by paste volume
Calcium hydroxide from cement hydration	8 to 10 percent by paste volume
Pozzolans, Slag, etc.	Distributed throughout the paste are fine, spherical clear to light to dark brown to black glassy particles of fly ash having the fineness of Portland cement
Water-cement ratio (*w/c*), estimated	0.45

Properties and Compositions of Paste	Concrete Cylinder
Portland cement contents, estimated (equivalent to bags of Portland cement per cubic yard)	7 1/2 to 8 bags of Portland cement per cubic yard, of which 20 percent is estimated to be fly ash
Secondary Deposits	None
Depth of Carbonation, mm	None
Microcracking	None except the ones formed from strength testing
Aggregate-paste Bond	Moderately tight to weak
Bleeding, Tempering	None
Chemical deterioration	None

Table 2: Proportions and compositions of hardened cement paste.

AIR

Air occurs as: (i) numerous fine discrete, spherical and near-spherical voids having sizes of up to 1 mm, and (ii) a few coarse, near-spherical and irregularly shaped voids of sizes coarser than 1 mm. The former voids are characteristic of entrained air and the latter ones are characteristic of entrapped air. Air content is 'estimated' from petrographic examinations to be 8 to 10 percent, which is higher than the reported maximum design air content of 7.5 percent.

Air-void analyses on lapped section of cylinder was done by the modified point count method of ASTM C 457. This study showed an air content of 8.1 percent, a void frequency of 29.68/in, an air-void specific surface of 1463 in^2/in^3 and a void spacing factor of 0.0029 in. Air-void parameters are indicative of a very 'fine' air-void system of high specific surface (noticeably higher than the common industry-recommended minimum value of 600 in^2/in^2), but an excessively air-entrained concrete that has numerous fine discrete spherical entrained voids to provide the necessary freeze-thaw durability of concrete but have more than necessary air to negatively affect the compressive strength. The following Table summarizes result of air-void analysis of lapped cross section of the core.

Air-Void Systems and Parameters	Concrete Cylinder
Air-Void System	Excessively Air-Entrained
Total Air Content, %, Determined	8.12
Specific Surface	1463
Void Frequency	29.68
Spacing Factor	0.0029
Paste-Air Ratio	4.24

Table 3: Air-void analysis of concrete.

DISCUSSIONS

REASONS FOR LOWER-THAN-DESIGN COMPRESSIVE STRENGTH OF CONCRETE

Therefore, based on detailed petrographic examinations and air-void analyses of concrete in the cylinder the reported lower-than-design compressive strength of concrete is found to be due to excessive air entrainment in concrete having 8.12 percent total air, in excess of the maximum design air content of 7.5 percent, and, more importantly, having other detrimental effects of excessive fine air bubbles, e.g., clustering of air along aggregate-paste interfaces to reduce the bonds and thereby reduce the strength. Although the 6-day strength result of this particular cylinder do not show any negative effect, such high air can explain the reported inconsistent strength results in the project.

REFERENCES

ASTM C 856 "Standard Practice for Petrographic Examination of Hardened Concrete," Vol. 4.02, ASTM International, West Conshohocken, PA, 2014.

Jana, D., Erlin, B., and Pistilli, M., "A Closer Look at Entrained Air in Concrete," *Concrete International*, American Concrete Institute, June 2005, pp. 31-38.

Jana, D., "Sample Preparation Techniques in Petrographic Examinations of Construction Materials: A State-of-the-art Review," *Proceedings of the 28th Conference on Cement Microscopy*, International Cement Microcopy Association, Denver, Colorado, pp. 23-70, 2006.

Jana, D., "A Round Robin Test on Measurements of Air Void Parameters in Hardened Concrete by Various Automated Image Analyses and ASTM C 457 Methods," *Proceedings of the 29th Conference on Cement Microscopy*, 2007, pp. 34-69.

✪ ✪ ✪ END OF TEXT ✪ ✪ ✪

END OF REPORT[1]

[1] The CMC logo is made using a lapped polished section of a 1930's concrete from an underground tunnel in the U.S. Capitol.